Journal of Propulsion and Power, Volume 33, Issue 5, September 2017
DOI: 10.2514/1.B35912

Creep Life Usage Analysis and Tracking for Industrial Gas Turbines

E.G. Saturday, Y. G. Li and E.A. Ogiriki

Centre for Propulsion Engineering, School of Aerospace, Transport and Manufacturing, Cranfield University, Bedfordshire, MK43 0AL, United Kingdom

M. A. Newby

Manx Utilities, Douglas, Isle of Man, United Kingdom

Abstract

Creep life usage analysis and tracking of first stage turbine rotor blades of an aero-derivative industrial gas turbine engine is investigated in this study. An engine performance model is created while blade thermal and stress models are developed for the calculation of the blade material temperatures and stresses at different sections of the blade. A creep life model is developed based on the Larson-Miller Parameter method by taking inputs from the thermal and stress models. An integrated creep life estimation system is developed by bringing together the engine performance model, the blade thermal and stress models, the creep life model and a data acquisition and pre-processing model. Relative creep life consumption analysis using new concepts developed in this research is introduced for the analysis of creep life consumption of the gas turbine engine operating for a period of time; these concepts include Equivalent Creep Life (ECL) and Equivalent Creep Factor (ECF). The developed algorithms have been applied to the creep life tracking of an aero derivative gas turbine engine using its field test data. The results show that it is able to provide a quick evaluation and tracking of engine creep life consumption and provide very useful information for gas turbine operators to support their operation optimization and creep life consumption monitoring.

Nomenclature

A = Cross-sectional area of blade (m^2)

A_n = Annulus area of the blade section (m^2)

BM_A = Bending moments in gas turbine axial direction

B_p = Blade perimeter (m)

BM_T = Bending moments in gas turbine tangential direction

BM_{XX} = Bending moments in blade axial direction

BM_{YY} = Bending moments in blade tangential direction

BM_{Ax}^V = Sum of velocity bending moments in gas turbine axial direction

BM_T^V = Sum of velocity bending moments in gas turbine tangential direction

c = Average chord of the blade

C_p = Specific heat capacity of cooling air

CF = Creep factor

CL = Creep life (hours)

ECF = Equivalent creep factor

ECL = Equivalent creep life (hours)

F = Force (N)

h_b = Blade height (m)

h_g = Heat transfer coefficient

I = Second moment of area

k_g = Thermal conductivity

LF = Life Fraction

m^* = Coolant mass flow function

$\dot{m}_c$ = Cooling mass flow rate (kg/s)

m_b = Mass of blade section (kg)

M = Bending moment

N_b = Number of blades

Nu_g = Nusselt number

Δp = Static pressure difference between blade suction and pressure sides

$\dot{Q}_{in}$ = Total energy input to the blade

$\dot{Q}_{out}$ = Total energy removed from blade

t_f = Stress rupture time (hours)

T = Temperature (K) or Time (hours)

x = Sum of life fraction

ε_{ff} = Overall cooling effectiveness

η_c = Convection cooling efficiency

θ = Blade stagger angle

σ = Bending stress

ω = Angular speed of the compressor shaft

Subscript:

Ax	=	Gas turbine axial direction
b	=	blade
c	=	coolant
CF	=	Centrifugal force
com	=	combustor
ex	=	exit
g	=	gas
G	=	Refers to LE, TE or SB
in	=	inlet
T	=	Gas turbine tangential direction
XX	=	Blade axial direction
YY	=	Blade tangential direction

Superscript:

MB	=	Bending moment
P	=	Pressure
Tot	=	Total
V	=	Velocity

I. Introduction

The hot section components, mainly the turbine rotor blades of gas turbines are exposed to very high temperature and very high rotational speed and are prone to failure in different modes. For industrial gas turbines operating under steady state operating conditions at most of the time, creep is a predominant failure mode. Several methods of assessing the creep life consumption of the creep-critical components, i.e. turbine blades of gas turbine engines, have been published [1–4] but the accuracy of the methods is of concern to both the manufacturers and the operators alike. Even the more elaborate finite element procedures for the analysis of creep life of engine components do not always give satisfactory results [5]. In view of this, it may be beneficial to develop a prediction method of relative creep life consumption by comparing the life consumption at any given engine operating condition to that at a reference operating condition. This may provide engine operators a different view on the engine creep life when the prediction of absolute engine creep life is not accurate.

Different time-temperature parameters have been introduced in the past to assess creep life consumption, such as Larson-Miller parameters (LMP) [6], Orr-Sherby-Dorn parameter (OSD) [7], Manson-Haferd parameters (MHP) [8] and Manson-Succop parameters (MSP) [9]. Among these parameters, Larson-Miller parameter is considered to be the most favourable one due to its ease of use and widespread applications and therefore it is adopted in this study.

Abdul Ghafir et al. [10-11] introduced the concept of Creep Factor (CF) to assess the impact of engine operations and health conditions on the creep life consumption of aero gas turbine hot section blades. In the paper, a novel accumulative creep life estimation method and a platform were introduced for quick assessment of blade life consumption using the Larson-Miller parametric method [6]. Relative creep life consumption of the engine operating at different scenarios has been estimated.

In this paper, new concepts of Equivalent Creep Life (ECL) and Equivalent Creep Factor (ECF) have been introduced and an integrated creep life estimation system has been developed in order to provide gas turbine users more effective creep life consumption indicators based on relatively simple models. They have been applied to the creep life consumption and tracking of an aero derivative industrial gas turbine engine running in Manx Utilities' power plant located in Isle of Man in the UK using engine field data. Prediction results have been presented and corresponding conclusions have been made.

II. Life Estimation Models and Methodology

The creep life estimation and accumulative creep life tracking process requires the creation of an engine thermodynamic performance model, a creep life prediction model, a blade thermal model and a blade stress model of gas turbine engines. Therefore an integrated creep life estimation system has been developed in this study for the creep life estimation and tracking of creep-critical components of gas turbine engines. This system and the relevant models are described in the following sections.

Integrated Creep Life Estimation System

The developed integrated creep life estimation system is shown in Fig. 1. A data acquisition and pre-processing model receives engine field data, pre-processes the data and sends them to the engine thermodynamic model that predicts the details of corresponding engine performance. The relevant performance data are then sent to the blade thermal and stress models that calculate the temperatures and stresses of the blades respectively, which are required by the creep life model to further predict the creep life consumption of the blade.

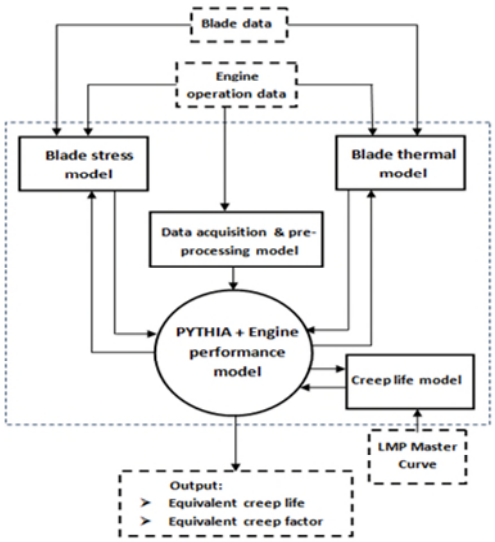

Fig. 1 Integrated Creep Life Estimation System

The five models that form the integrated creep life estimation system are enclosed by dotted lines, while the input data to the system and the output results from the system are placed outside the system. Engine field data including the measurements of pressures, temperatures, shaft rotational speed, fuel flow rate, power output, etc. recorded continuously over time are used as input to the system. The major outputs of the system are the Creep

Factors and the Creep Lives for individual points of engine operation, and the Equivalent Creep Life (ECL) and the Equivalent Creep Factor (ECF) for an entire period of engine operation.

Creep Life Model

The Larson-Miller Parameter (LMP) model [6] is used for the creep life analysis in this study. It is given by Eq. (1).

$$t_f = 10^{\left(\frac{LMP}{T_b} - C\right)} \tag{1}$$

where t_f is stress rupture time or time to failure in hours, T_b is blade material temperature in *K*, *C* is material constant usually being of the order of 20, and *LMP* is the Larson-Miller Parameter. The temperature here refers to blade material temperature upon which the blade life is determined and can be predicted by the blade thermal model. The *LMP* value depends on the stress of the blade and blade material property. The blade stress may be obtained from the stress model while the value of the *LMP* can be obtained by interpolation of a *LMP* master curve. Depending on the value of the Larson Miller Parameter it may be divided by 1000 when plotting the master curve and therefore Eq. (1) may be replaced by Eq. (2)

$$t_f = 10^{\left(\frac{1000 \times LMP}{T} - C\right)} \tag{2}$$

The accuracy of the prediction using Eq. (1) or (2) relies on the LMP master curve of the blade material, the blade metal temperature and the assumption of the constant C value. The material constant C typically takes a value between 17 and 23 and the value of 20 is used in most engineering applications and therefore *C=20* is used in this study. As the above assumptions may result in prediction errors in the estimation of absolute blade life, a relative life consumption analysis is investigated in this study with the intention of providing gas turbine users a different view of engine creep life consumption. The details of such development are described later in the paper.

Blade Thermal Model

A blade thermal model is developed to estimate the temperature of various sections of a blade. It is based on overall energy continuity across the blade with the consideration of heat transfer between hot gas traversing the blade and cooling air passing through a cooling channel inside the blade from blade root to blade tip. It is assumed that the cooling air comes from the exit of the upstream compressor. To simplify the prediction, the blade is divided into 8 equal sections along the span where 9 nodal temperatures are estimated using convective

cooling. A radial temperature distribution along the blade span may look like the one shown in Fig. 2, which is mainly determined by the air and fuel distribution of upstream combustor [12]. It is also assumed in this study that a single pass internal cooling within the blade is considered and a simplified cooling configuration is shown in Fig. 3.

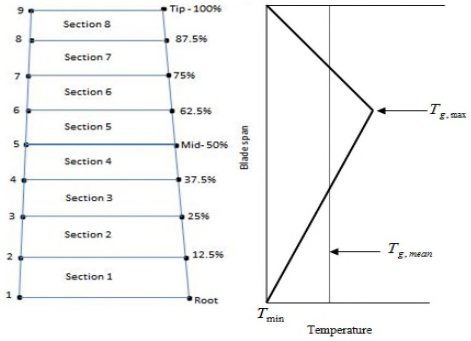

Fig.2 Blade Sections and Inlet Radial Temperature Distribution

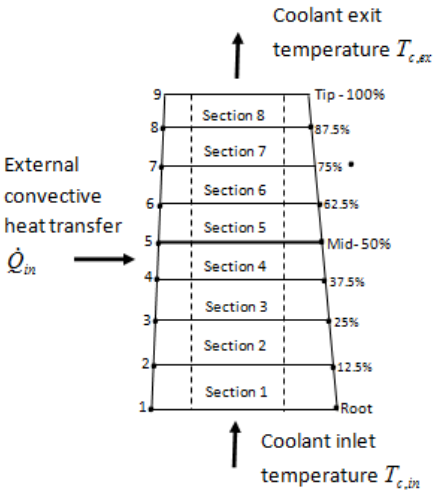

Fig. 3 Heat Transfer and Coolant Temperatures around Turbine Blade

Three key parameters are employed in the blade thermal model. These are coolant mass flow function, overall cooling effectiveness and convective cooling efficiency [13]. Considering a single turbine blade, the energy input to the whole blade, $\dot{Q}_{in}$ is,

$$\dot{Q}_{in} = h_g B_p h_b \left(T_g - T_b\right) \tag{3}$$

where h_g is the external heat transfer coefficient, B_p the perimeter of the blade, h_b the blade height, T_g the gas temperature, and T_b the blade material temperature. As the creep life tracking is for existing engines, the geometric data of the blade is assumed to be available and used as input. In the cases where the blade geometry cannot be easily obtained, such as that in this study, a blade sizing method using constant mean diameter method described in [11] may be used to estimate the blade geometry and therefore h_b and B_p may be obtained.

The external heat transfer coefficient h_g is calculated for each blade section, and it is given by Eq. (4)

$$h_g = \frac{Nu_g \times k_g}{c} \tag{4}$$

where Nu_g is the Nusselt number of the gas, k_g the thermal conductivity of the gas and c the average chord of the blade section. Details of the estimation of the external heat transfer coefficient could be found in [14].

The energy removed from the whole blade, $\dot{Q}_{out}$ is given by Eq. (5)

$$\dot{Q}_{out} = \dot{m}_c C_p \left(T_{c,ex} - T_{c,in}\right) \tag{5}$$

where C_p is the specific heat capacity of the cooling air, $\dot{m}_c$ the coolant mass flow rate, $T_{c,in}$ the coolant in-flow temperature and $T_{c,ex}$ the coolant exit temperature. Under steady state operating conditions, the energy input to the whole blade is equal to the energy removed from the blade and therefore Eq. (6) may be obtained from Eqs. (3) and (5),

$$m^* = \frac{\dot{m}_c C_p}{h_g B_p h_b} = \left(\frac{T_g - T_b}{T_{c,ex} - T_{c,in}}\right) \tag{6}$$

where m^* is a non-dimensional representation of the coolant mass flow. The overall cooling effectiveness, ε_{ff} and the convection cooling efficiency, η_c are given respectively by Eqs. (7) and (8).

$$\varepsilon_{ff} = \frac{T_g - T_b}{T_g - T_{c,in}} \tag{7}$$

$$\eta_c = \frac{T_{ex} - T_{c,in}}{T_b - T_{c,in}} \tag{8}$$

Therefore,

$$\varepsilon_{ff} = \frac{m * \eta_c}{1 + m * \eta_c} \tag{9}$$

Although ε_{ff} varies across the blade height it is assumed to be constant for simplicity and may take the value of about 0.5 [12].

Based on the definition of radial temperature distribution factor (RTDF) [15], the maximum radial gas temperature $T_{g,\max}$ at the combustor exit or the turbine inlet may be estimated by Eq. (10)

$$T_{g,\max} = T_{g,mean} + RTDF * \left(T_{g,mean} - T_{com,in}\right) \tag{10}$$

where $T_{com,in}$ is the combustor inlet mean temperature and $T_{g,mean}$ is the turbine inlet mean temperature, both of which can be obtained from the engine performance model created in PYTHIA [16], a gas turbine thermodynamic performance and gas path diagnostics software developed and validated [17] at Cranfield University. It is recommended that the RTDF may take a value less than 0.2 [18] so the RTDF value of 0.12 is used in this study. It is further assumed that $T_{g,\max}$ occurs at 62.5% blade height [12], the minimum gas temperatures occur at both the blade root and the blade tip, and the temperature distributions from the location of the maximum temperature to both the blade root and the blade tip are linear. Such assumption is based on the consideration that the air cooling effectiveness is better around the middle of the blade than that at both ends, blade centrifugal load decreases from blade root to blade tip and the blade creep life is determined by both the mechanical and thermal stresses of the blade. Therefore, all nodal temperatures can be estimated, and the minimum gas temperature $T_{g,\min}$ can be obtained with Eq. (11).

$$T_{g,\min} = \frac{9T_{g,mean} - 4T_{g,\max}}{5} \tag{11}$$

With Eq. (6), the metal mean temperature at blade section *i*, $T_{b,i}$ can be obtained with Eq. (12)

$$T_{b,i} = T_{g,i} - \varepsilon_{ff}\left(T_{g,i} - T_{c,in,i}\right) \tag{12}$$

Combining Eqs. (6) and (7) and applying them to a blade section, the coolant exit temperature of section *i* can be calculated by Eq. (13).

$$T_{c,ex,i} = T_{c.in,i} + \frac{h_{g,i}\, B_{P,i} h_{b,i} \times \varepsilon_{ff} \left(T_{g,i} - T_{c,in,i}\right)}{\dot{m}_c \times C_p} \tag{13}$$

Blade Stress Model

The blade stress model calculates the stresses at different locations along the span of the blade and evaluates the maximum stress on the blade. In other words, at different span locations stresses are evaluated at the leading edge (LE), the trailing edge (LE) and the furthest point at the blade suction surface indicated as (SB) because they are the most likely places for the maximum stress [10]. The stress model incorporates the centrifugal stresses due to blade rotation and the bending moment stresses due to pressure difference and velocity difference along the span. The centrifugal force $F_{CF,i}$ generated by each blade section is calculated by Eq. (14).

$$F_{CF,i} = m_{b,i} \times \omega^2 \times h_{CG,i} \tag{14}$$

where m_i is the mass of the section, ω the angular speed of rotation, and $h_{CG,i}$ the distance from the centre of gravity of the section to the turbine axis of rotation. The angular speed ω is obtained from Eq. (15),

$$\omega = \frac{2\pi N}{60} \tag{15}$$

where N is the rotational speed of the blade obtained from the performance model in PYTHIA. The total centrifugal force at node i may be given by Eq. (16),

$$F^{i}_{CF} = \sum_{s=i}^{8} F_{CF,s} \tag{16}$$

The centrifugal stress at each node $\sigma_{CF,i}$ may be given by Eq. (17) where A_i is the cross-sectional area of the blade at node i.

$$\sigma_{CF,i} = \frac{F^{i}_{CF}}{A_i} \tag{17}$$

The pressure bending moment BM_i^P on each node may be calculated by Eq. (18)

$$BM_i^P = F_{P,i} \times \frac{h_{b,i}}{2} \tag{18}$$

where $h_{b,i}$ is the height of blade section *i* and $F_{P,i}$ the pressure force acting at the centre of gravity of the blade section, given by Eq. (19),

$$F_{P,i} = \frac{\Delta p \times A_{n,i}}{N_b} \tag{19}$$

where N_b is the number of blades, $A_{n,i}$ the annulus area of the blade section and Δp the static pressure difference between the suction and pressure sides of the blade. Gas flow velocity changes in both the axial and the tangential directions resulting in axial velocity bending moment, $M_{Ax,i}^V$ and tangential velocity bending moment, $M_{T,i}^V$ about the centre of gravity of each blade section given by Eq. (20) and Eq. (21) respectively,

$$M_{Ax,i}^V = F_{Ax,i}^V \times \frac{h_{b,i}}{2} \tag{20}$$

$$M_{T,i}^V = F_{T,i}^V \times \frac{h_{b,i}}{2} \tag{21}$$

where $F_{Ax,i}^V$ is the axial component of the momentum force and $F_{T,i}^V$ is the tangential component of the momentum force that may be calculated with gas mass flow rate and velocity components in both directions. The axial and tangential directions are shown in Fig. 4.

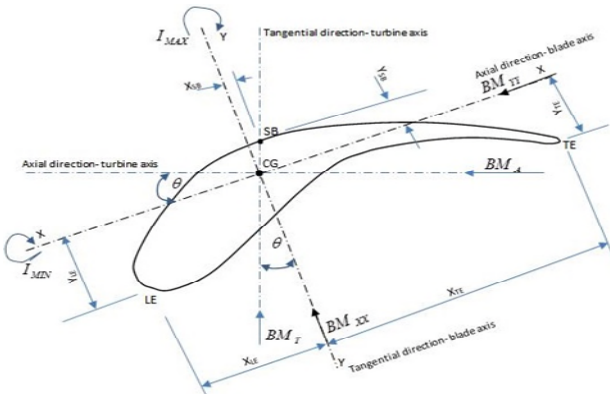

Fig. 4 Bending Moments Relative to Turbine Axis and Blade Directions

The gas velocities over the blade are calculated based on mass continuity at the inlet and the exit of the blade row and they are mainly determined by the shape of the blades. The sums of the velocity bending moments at the root of blade section i in the axial and the tangential directions are given by Eqs. (22) and (23) respectively.

$$BM^{V}_{Ax,i} = \sum_{i=i}^{i=8} M^{V}_{Ax,i} \tag{22}$$

$$BM^{V}_{T,i} = \sum_{i=i}^{i=8} M^{V}_{T,i} \tag{23}$$

The total bending moments can then be calculated by Eqs. (24) and (25)

$$BM_{XX,i} = \left(BM_{P,i} + BM^{V}_{Ax,i}\right)\cdot \sin\theta_i + BM^{V}_{T,i}\cdot \cos\theta_i \tag{24}$$

$$BM_{YY,i} = \left(BM_{P,i} + BM^{V}_{Ax,i}\right)\cdot \cos\theta_i - BM^{V}_{T,i}\cdot \cos\theta_i \tag{25}$$

where $BM_{XX,i}$ and $BM_{YY,i}$ are the axial and the tangential bending moments on the blade section i respectively, and θ is the blade stagger angle which may vary from the blade tip to the root. The bending moment stresses at the three chord-wise locations of blade section *i* are given by Eq. (26),

$$\sigma^{BM}_{G,i} = \frac{BM_{XX,i}\times Y_{G,i}}{I_{XX,i}} + \frac{BM_{YY,i}\times X_{G,i}}{I_{YY,i}} \tag{26}$$

where $\sigma^{BM}_{G,i}$ is the bending moment stress, the subscript *G* indicates the location of the blade section surface (i.e. leading edge *LE*, training edge *TE* or the farthest point *SB* at the blade suction surface), I_{XX} is the second moment of area about the blade axial direction, I_{YY} the second moment of area about the blade tangential direction, and $X_{G,i}$ and $Y_{G,i}$ the distances between the centre of gravity and the respective three locations indicated by *G*. It is worth mentioning that once the blade shape becomes available both I_{XX} and I_{YY} can be estimated and in this study I_{XX} =8.14*10^{-8} m^4 and I_{YY} =4.78*10^{-8} m^4. The total stress $\sigma^{Tot}_{G,i}$ at each of the three locations at the root of each blade section is

$$\sigma^{Tot}_{G,i} = \sigma_{CF,i} + \sigma^{BM}_{G,i} \tag{27}$$

The maximum stress $\sigma_{\max,i}$ at the root of each section of the blade is the maximum value of the three stresses at the root of each section, Eq. (28).

$$\sigma_{\max,i} = \max\left(\sigma_{G,i}^{Tot}\right) \tag{28}$$

Thermal stresses may also have impact on blade life particularly at transient process. They are not considered in this study as the focus of this study is on creep life consumption of industrial gas turbines normally working at steady state most of the time. The impact of thermal stresses on creep life may be investigated in future research.

Life Fractions and Equivalent Creep Life

Based on the above models, the creep life estimation model for the turbine blade at different engine operating conditions has been developed. The creep life of all blade sections is estimated and the lowest creep life is taken as the creep life of the whole blade. It is assumed that a period of engine operation can be divided into a series of time spans where in each span the engine is operated at same ambient and operating condition. The Life Fraction concept [19] is used in this study and at each operation time span the Life Fraction is defined by Eq. (29),

$$LF_i = \frac{T_i}{CL_i} \tag{29}$$

where T_i is the operating time at the time span i, and CL_i the creep life corresponding to the operating condition in the time span. Employing Robinsons life fraction rule [18], the sum of the Life Fractions *x* for a period of engine operation can be expressed by Eq. (30)

$$x = \sum_{i=1}^{m} LF_i = \sum_{i=1}^{m} \frac{T_i}{CL_i} \tag{30}$$

where m is the number of the time spans and $x \le 1$. Blade failure will occur when the sum of Life Fractions is accumulated to unity, i.e. $x = 1$.

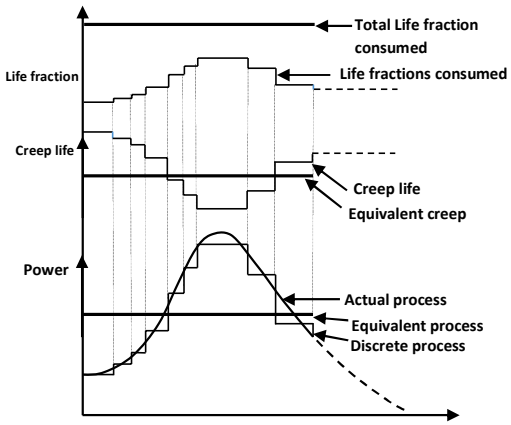

Fig.5 Actual and Equivalent Operation Processes

The concept of Life Fraction is very useful for gas turbine users to assess the amount of creep life that has been consumed for a complicated operation process. The higher the creep life for a given period of engine operation, the smaller the Life Fraction consumed. However, the users may also be keen to know how quickly the creep life has been consumed for an operation process. Therefore, a new concept of Equivalent Process and Equivalent Creep Life for an engine operating process is introduced as follows.

A schematic of a discrete process of an engine operation and its corresponding creep life and Equivalent Process is shown in Fig. 5. In other words, if an engine operates in a process with a constant ambient and operating condition and the process takes the same total operating time and consume the same Life Fraction as that of an actual operation process, the former process is called the Equivalent Process of the later and the creep life of such an Equivalent Process is called Equivalent Creep Life (*ECL*). Such a concept of *ECL* represented by Eqs. (31) and (32) has the advantage that the creep life of a complicated process can be represented by a single Equivalent Creep Life, which is a more useful life consumption indicator for gas turbine users.

$$x = \sum_{i=1}^{m} \frac{T_i}{CL_i} = \frac{\sum_{i=1}^{m} T_i}{ECL} \tag{31}$$

$$ECL = \frac{\sum_{i=1}^{m} T_i}{\sum_{i=1}^{m} \frac{T_i}{CL_i}} \tag{32}$$

The Equivalent Creep Life (*ECL*) of an engine is calculated by tracking an entire complicated operating process of an engine using the system shown in Fig. 1 based on the measurement of ambient condition and shaft power output of the engine during the whole process. *ECL* is able to indicate how quickly the engine creep life is consumed for a complicated engine operation process. A large value of ECL indicates slow life consumption, and vice versa.

Creep Factor and Equivalent Creep Factor

The Creep Factor CF_i [10] is defined as the ratio between the creep life at a given engine operating condition to that at a user-defined reference operating condition and can be represented by Eq. (33)

$$CF_i = \frac{CL_i}{CL_{\mathrm{Re}\,f}} \tag{33}$$

where CL_i is the creep life at a certain operating condition and $CL_{\mathrm{Re}\,f}$ is the creep life at a user-defined reference operating condition. For a period of engine operation, shown in Fig.6, the Creep Factor represents the speed of creep life consumption at a certain operation condition at a particular moment relative to that at a reference operating condition.

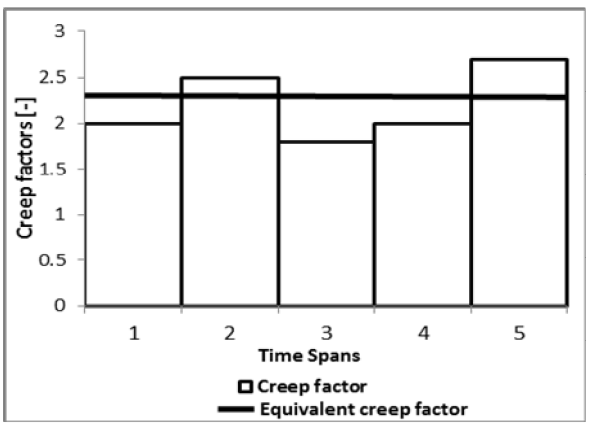

Fig.6 Creep Factors and Equivalent Creep Factor in a Period of Engine Operation

In order to represent the speed of creep life consumption for a period of engine operation a new concept of Equivalent Creep Factor (*ECF*) is introduced in this study. It is defined as the ratio between the Equivalent Creep Life for a period of engine operation and the creep life at a user-defined reference engine operating condition and can be represented by Eq. (34).

$$ECF = \frac{ECL}{CL_{\mathrm{Re}\,f}} \tag{34}$$

The Equivalent Creep Factor (ECF) for a time period may be obtained from the Creep Factors of all time spans in the same time period, Eqs. (35) and (36).

$$ECF = \frac{ECL}{CL_{\mathrm{Re}\,f}} = \frac{\sum_{i=1}^{m} T_i}{\sum_{i=1}^{m} \frac{T_i}{CL_i}} \times \frac{1}{CL_{\mathrm{Re}\,f}} \tag{35}$$

$$ECF = \frac{\sum_{i=1}^{m} T_i}{\sum_{i=1}^{m} \frac{T_i}{CF_i}} \tag{36}$$

The Equivalent Creep Factor (ECF) is a non-dimensional parameter indicating the rate of engine creep life consumption relative to that at a reference operating condition. ECF of unity means the cumulative effect of the engine operation on creep life for the period of operation is the same as that of the engine operating at the reference condition. ECF greater than unity portrays a favourable engine operation with respect to the reference condition, i.e. the time to creep failure is longer than the reference creep life; and vice versa. It offers benefits to gas turbine operators to monitor the rate of engine life consumption over the whole process and compensate to the Creep Factor (CF) that indicates the rate of creep life consumption at any moment. The usage of the Equivalent Creep Factor, combined with the usage of Creep Factor, allows gas turbine users to monitor whether the engine is being used at favourable conditions, identify critical parts of the process where engine creep life is consumed the most and assists the operators to minimize creep life consumption while keeping required power generation.

III. Creep Life Tracking: Case Study

The above lifing model and system has been applied to an aero derivative industrial gas turbine engine operated in Manx Utilities, Isle of Man, UK to track the creep life consumption of the engine.

Engine Model Creation and Model Adaptation

The gas turbine engine used in this study is a GE LM2500+ aero derivative gas turbine engine. It is a twin shaft engine with a compressor, a combustor, a compressor turbine and a free power turbine. The creep life of the first

stage rotor blades of the compressor turbine is targeted in this study. A thermodynamic performance model of the engine is created in PYTHIA software [16]. The engine model configuration is shown in Fig. 7 while the basic engine performance specification at sea level ISA condition [20] is shown in Table 1.

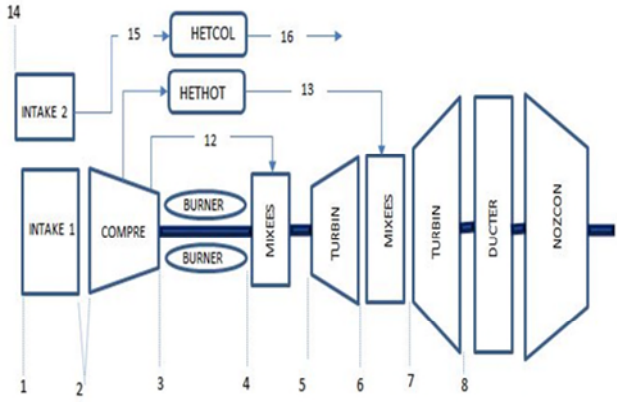

Fig.7 Engine Model Configuration

Table 1 Engine Performance Specification at Sea Level ISA Condition [20]

No.	Parameter	Unit	Value
1	Power output	MW	30.2
2	SFC	g/kW-hr	212
3	Heat rate	kJ/kWs-hr	9227
4	Exhaust gas flow	Kg/s	85.9
5	Exhaust gas temp.	^{o}C	518
6	Power turbine speed	rpm	3600

The thermodynamic performance model has been adapted to the real engine at both design and off-design operating conditions by using the adaptation method developed at Cranfield [21]–[23] and the field data of the engine. This is to ensure that the model provide accurate performance predictions that will be used for lifing analysis. Fig. 8 shows a comparison of the power turbine exit temperature, T8 over a period of one day operation between the real engine measurements and the simulated results from the adapted engine model. The figure shows that the simulated data march the field data very well and the maximum prediction error during the period is less than 0.02%. This demonstrates that the accuracy of the created engine performance model is satisfactory.

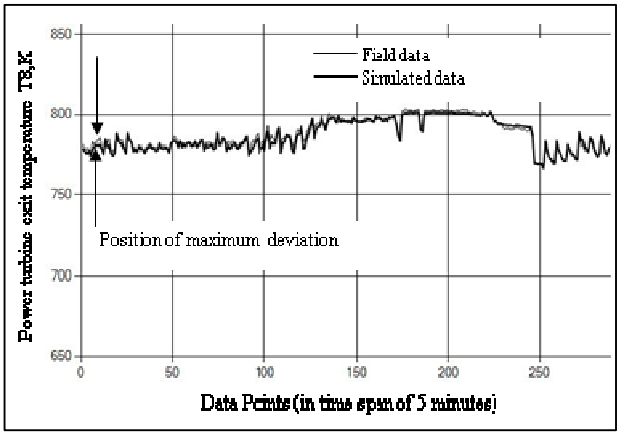

Fig. 8 Comparison of Field and Simulated Data

The actual engine operation data on a typical day of four typical months (January, February, June and July of a year) is used in the case study for the testing of the creep life analysis system. The engine shaft power output indicates the operating condition of the engine and is used as the handle (power setting parameter) of the engine performance model.

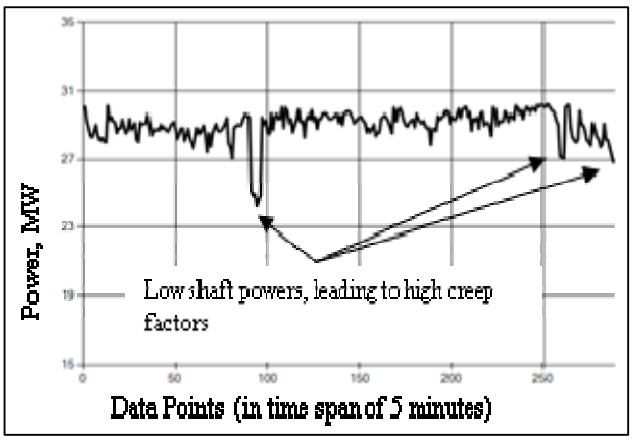

Fig.9 Engine Shaft Power Variations

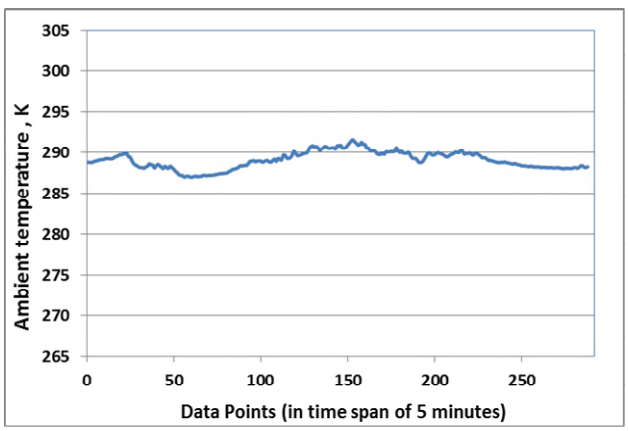

Fig. 10 Ambient Temperature Variations

As the engine operating condition is dominated by the shaft power output and the ambient temperature, the variations of these two parameters over time on a typical day in June in the UK are selected and shown in Figs. 9 and 10. The impact of ambient pressure and humidity is ignored as their impact on engine performance and creep life is much smaller. Fig. 11 shows a comparison among the predicted Creep Life, the Life Fraction and the Equivalent Creep Life over the typical day of engine operation. Due to several assumptions, such as the blade geometry assumed to be rectangular, linear temperature distributions between blade root and tip, blade material being Rene 80 with density of 7800kg/m^3, Larson-Miller Parameter constant being 20, estimated LMP values, etc. may not be accurate enough, the predictions of blade creep life, the Equivalent Creep Life and the Life fractions may also not be accurate enough in absolute terms. Therefore, the introduced Creep Factor and Equivalent Creep Factor showing relative creep life consumption against a user-defined reference condition may provide a different view of creep life consumption for gas turbine users. For that reason, only results using Creep Factor and Equivalent Creep Factor are presented in the following analysis.

In this study, the reference operating condition is specified at engine shaft power being 30MW, blade rotational speed 9780 rpm, ambient temperature 13^{o}C, ambient pressure 1 atm and relative humidity 68%. Such a reference operating point was selected from engine test data with the consideration that it is close to engine maximum power output and also close to standard ISA condition at sea level.

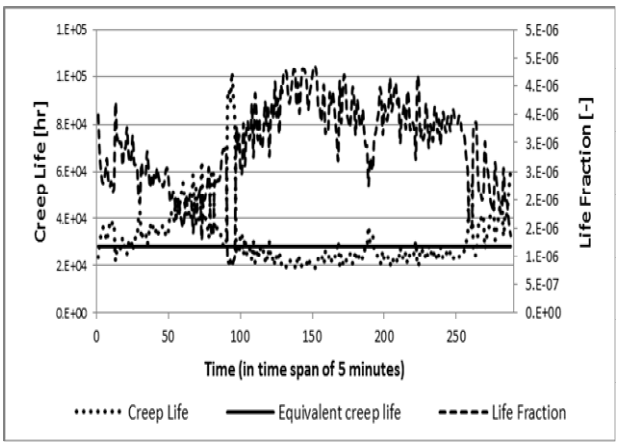

Fig. 11 Predicted CL, ECL and LF for a Typical Day Operation

The predicted Creep Factors of the engine for a typical day of operation is shown in Fig. 12. It can be seen that the Equivalent Creep Factor being 1.09 for the day is above the Creep Factor being 1.0 at the reference condition, indicating that the overall operation of the engine was on the favourable side in terms of creep life consumption and the engine creep life consumption is 9% lower than that at the reference operating condition.

The high Creep Factor values around data point 90 shown in Fig.12 are due to low engine operating conditions indicated by the low power output at the same data points shown in Fig. 9.

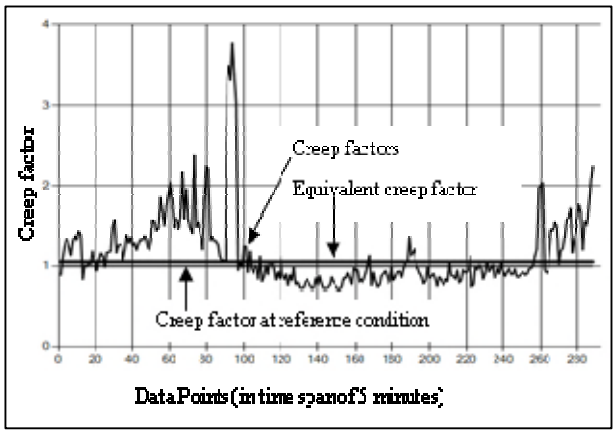

Fig. 12 Creep Factors and Equivalent Creep Factor for a Typical Day of Engine Operation

The same analysis has also been applied to a longer period of engine operation to track the engine life consumption. This is demonstrated in the following life tracking of the blades for a period of four months using actual engine operation data, Table 2.

Table 2 Data for Creep Life Analysis

S/No.	Month	No. of days used
1	January	27
2	February	22
3	June	27
4	July	26

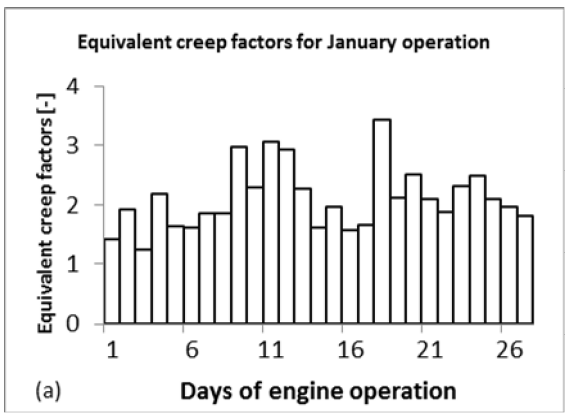

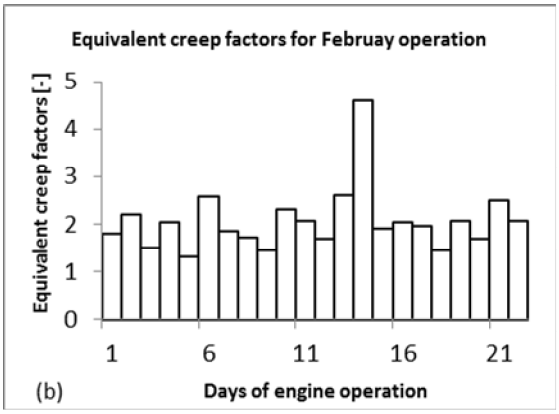

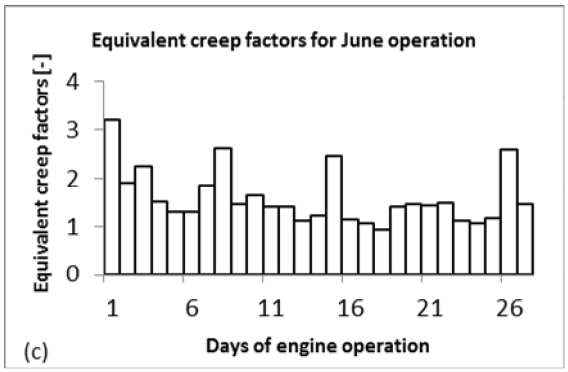

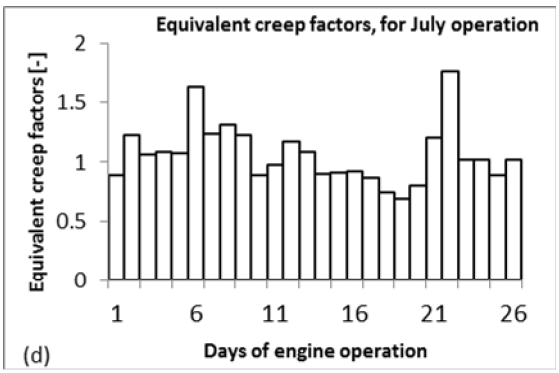

Fig. 13 Equivalent Creep Factors in Different Months of Engine Operation

The daily Equivalent Creep Factors of the engine operation for the four months are shown in Fig. 13. It can be seen in Fig. 13 (a) and (b) that the Equivalent Creep Factors per day in January and February are all above 1, indicating more favourable engine operation compared with that at the reference operating condition. This was due to low ambient temperatures at similar level of engine shaft power output. The Equivalent Creep Factors in June shown in Fig. 13(c) become lower than those in January and February due to higher ambient temperature and at similar power level. As the Equivalent Creep Factors in June are still higher than 1.0, the overall impact on creep life is still favourable compared with that at the reference operating condition. In July, as depicted in Fig.13 (d), the engine was operated at even higher ambient temperature and produced similar power output so

the Equivalent Creep Factors were lower than unity in some of the days. This indicates that the engine operation in hot days is no longer favourable in term of creep life consumption compared with that at the reference operating condition. Based on the above analysis, to mitigate fast consumption of the engine creep life in hot days, the engine operator may use the Creep Factor analysis as a guidance to slightly reduce the engine power level or keep the same power output but use inlet fogging for the sake of saving engine creep life.

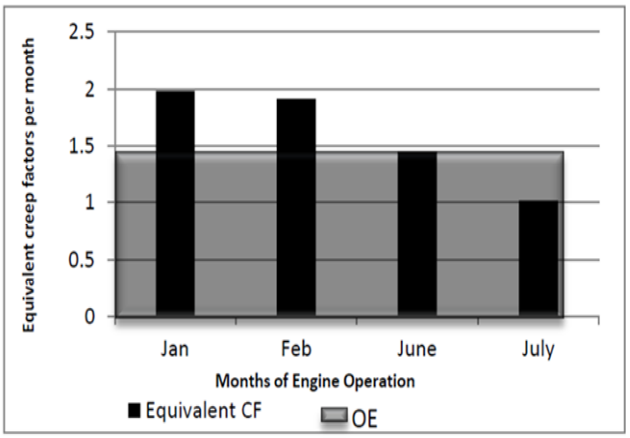

Fig. 14 Comparison of Equivalent Creep Factors for Different Months of Engine Operation

A better global image of the engine creep life consumption may be obtained by calculating the Equivalent Creep Factor for each month of the engine operation or even for the whole four month period as that shown in Fig. 14. It can be seen in Fig. 14 that the monthly Equivalent Creep Factor is decreasing from January to July due to similar power output but increasing ambient temperature over the time. Based on the predicted monthly Equivalent Creep Factors, it can be seen that January and February operation was the most favourable with an Equivalent Creep Factor being around 2, indicating that the life consumption rate is about half of that at the reference operating condition. July is the worst time of engine operation with monthly Equivalent Creep Factor being about 1 indicating the same rate of creep life consumption as that at the reference operating condition. The overall Equivalent Creep Factor indicated by "OE" in the Figure for the whole four month period is around 1.47, indicating that the creep life consumption rate is 47% less than that at the reference operating condition.

As the above results are predicted by a physics-based creep life estimation model, the impact of the relative creep life consumption due to the variation of ambient temperature and engine operating conditions should be estimated with good confidence although prediction errors are inevitable. Such analysis may provide gas turbine uses an alternative view of engine creep life consumption to support creep life monitoring and optimize engine operations without jeopardizing engine safety.

IV. Conclusions

In this paper, new concepts of Equivalent Process of engine operation, Equivalent Creep Life (ECL) and Equivalent Creep Factor (ECF) are introduced and a creep life analysis system including a thermal model, a stress model, an engine thermodynamic performance model and a creep life estimation model has been developed for engine creep life consumption analysis. The advantage of using these new concepts is to enable gas turbine users to quantitatively assess engine creep life consumption against that at a user-defined reference operating condition in order to monitor engine creep life consumption, evaluate if the operation is favourable and optimize engine operations when accurate absolute creep life consumption is difficult to obtain. A case study has been carried out to apply the developed creep life estimation method and system to a LM2500+ engine operated in Manx Utilities, Isle of Man in the UK using the field data of four different months to test the applicability of the developed new concepts and system. Results show that at similar level of engine power output the Equivalent Creep Factors are around 2 in January and February when ambient temperatures were low and around 1 when ambient temperatures were high in July. This indicates that the blade creep life consumption rate in January and February is half of that at the reference operating condition and almost the same in July as that at the reference operating condition. The overall Equivalent Creep Factor for the whole four months is 1.47, indicating that the creep life consumption rate is around 47% less than that at the reference operating condition. The case study shows that the developed new method may be able to provide a quick evaluation and tracking of relative engine creep life consumption and provide very useful information to support gas turbine users in their creep life monitoring and operation optimization.

Acknowledgement

The authors express their gratitude to the Niger Delta Development Commission (NDDC), Nigeria, and Manx Utilities (MU), Isle of Man, UK for sponsoring this research. The authors also thank Mr Graham Stigant at Manx Utilities for providing engine field data and technical support.

References

[1] M. Vaezi and M. Soleymani, “Creep Life Prediction of Inconel 738 Gas Turbine Blade,” *Journal of Applied Sciences*, vol. 9, no. 10, pp. 1950–1955, 2009.

[2] G. Marahleh, A. R. I. Kheder, and H. F. Hamad, “Creep-Life Prediction of Service-Exposed Turbine Blades,”

Materials Science, vol. 42, no. 4, pp. 476–481, Jul. 2006.

[3] M. Naeem, “Implications of day Temperature Variation for an Aero-engine’s HP Turbine-Blade's Creep Life-Consumption,” *Aerospace Science Technology*, vol. 13, pp. 27–35, 2009.

[4] Z. Kong and S. Li, “Effects of Temperature and Stress on the Creep Behavior of a Ni 3 Al Base Single Crystal Alloy,” *Progress in Natural Science: Materials International*, vol. 23, no. 2, pp. 205–210, 2013.

[5] Z. Liu, D. N. Mavris, and V. Volovoi, “Creep Life Prediction of Gas Turbine Components Under Varying Operating Conditions”, JPGC2001/PWR-19163, *ASME International Joint Power Generation Conference, June 4-7, New Orleans, Louisiana*, USA, June 2001.

[6] F. R. Larson and J. Miller, “A Time-Temperature Relationship for Rupture and Creep Stresses,” *Transactions of ASME*, vol. 74, pp. 765–775, 1952.

[7] R. Orr, O. Sherby and J. Dorn, "Correlation of Reupture Data for Metals at Elevated Temperatures", Transactions of ASM, Vol. 46, pp.113-118, 1954.

[8] S.S. Manson and A.M. Haferd, "A Linear Time-Temperature Relation for Extrapolation of Creep and Stress Rupture Data", NACA TN 2890, 1953.

[9] S. Mnson and G. Succop, "Stress-Rupture Properties of inconel 700 and Correlation on the Basis of Several Time-Tempeature Parameters", Symposium on Metallic Materials for Service Temperatures Above 1600 F, ASTM-STP 174, ASTM, 1956.

[10] M. F. Abdul Ghafir, Y. G. Li, R. Singh, K. Huang, and X. Feng, “Impact of Operating and Health Conditions on Aero Gas Turbine Hot Section Creep Life Using a Creep Factor Approach”, *GT2010-22332, ASME Turbo Expo 2010, June 14-16*, 2010.

[11] M. F. Abdul Ghafir, Y. G. Li, L. Wang, and W. Zhang, “Impact Analysis of Aero-engine Performance Parameter Variation on Hot Section’s Creep Life Using Creep Factor Approach,” *AIAA Journal of Propulsion and Power*, vol. 16, no. 9, pp. 1–12, 2011.

[12] T. C. Lieuwen and Y. Vigor,, "Gas Turbine Emissions", Cambridge University Press, 2013.

[13] L. Torbidoni and J. H. Horlock, “A New Method to Calculate the Coolant Requirements of a High-Temperature Gas Turbine Blade,” *Journal of Turbomachinery*, vol. 127, pp. 191–199, 2005.

[14] H. I. H. Saravanamuttoo, G. F. C. Rogers, H. Cohen, and P. V Straznicky, *Gas Turbine Theory*, 6th ed. London: Pearson Educational Limited, 2009.

[15] A. H. Lefebvre, *Gas Turbine Combustion*, 2nd ed. Phiadelphia: Taylor and Francis, 1999.

[16] Y. G. Li and R. Singh, “An Advanced Gas Turbine Gas Path Diagnostic System-PYTHIA”, ISABE-2005-1284, *The XVII International Symposium on Air Breathing Engines, Munich, Germany*, 2005.

[17] J. Blinstrub, T.G. Li, M. Newby, Q. Zhou, G. Stigant, P. Pilidis and H Honen, “Application of Gas Path Analysis to Compressor Diagnosis of an Industrial Gas Turbine Using Field Data”, GT2014-25330, ASME TURBO EXPO 2014, Dusseldorf, Germany, June 2014.

[18] P. Walsh and P. Fletcher, "Gas Turbine Performance", 2nd ed. Oxford: Blackwell Publishing Company, 2004.

[19] S. L. Robinson, “Effect of Temperature Variation on the Long Time Rupture Strength of Steels,” *Transactions of ASME 74*, pp. 777–780, 1952.

[20] GE-Marine, “LM2500+ Marine Gas Turbine”, 2014. www.geaviation.com/engines/docs/marine/datasheet-lm2500plus.pdf. [Accessed on 20-Jan-2015].

[21] Y. G. Li, P. Pilidis, and M. A. Newby, “An Adaptation Approach for Gas Turbine Design-Point Performance Simulation,” *Journal of Engineering for Gas Turbines and Power*, vol. 128, no. 4, pp. 789–795, 2006.

[22] Y. G. Li, L. Marinai, V. Pachidis, E. Lo Gatto, and P. Pilidis, “Multiple-Point Adaptive Performance Simulation Tuned to Aeroengine Test-Bed Data,” *AIAA Journal of Propulsion and Power*, vol. 25, no. 3, pp. 635–641, 2009.

[23] Y. G. Li and P. Pilidis, “GA-Based Design-Point Performance Adaptation and its Comparison with ICM-Based Approach,” *Applied Energy*, vol. 87, no. 1, pp. 340–348, Jan. 2010.

Creep-life usage analysis and tracking for industrial gas turbines

Saturday, Egbigenibo Genuine

2017-07-14

Saturday EG, Li YG, Ogiriki EA, Newby MA. (2017) Creep-life usage analysis and tracking for industrial gas turbines. Journal of Propulsion and Power, Volume 33, Issue 5, September 2017, pp. 1305-1314

https://doi.org/10.2514/1.B35912